THE JOURNAL OF PHYSICAL CHEMISTRY LETTERS
A JOURNAL OF THE AMERICAN CHEMICAL SOCIETY

pubs.acs.org/JPCL

Letter

Fluorescence Quenching Dynamics of 2-Amino-7-methyl-1,8-naphthyridine in Abasic-Site-Containing DNA Duplexes for Nucleobase Recognition

Chunfan Yang, Fang Wang, Qian Zhou, Jialong Jie,* and Hongmei Su*

Cite This: *J. Phys. Chem. Lett.* 2023, 14, 10585−10591

Read Online

ACCESS | Metrics & More | Article Recommendations | Supporting Information

ABSTRACT: Dramatic fluorescence quenching of small heterocyclic ligands trapped in the abasic site (AP) of DNA has been implemented as an unprecedented strategy recognizing single-base mutations in sequence analysis of cancer genes. However, the key mechanisms governing selective nucleobase recognition remain to be disentangled. Herein, we perform fluorescence quenching dynamics studies for 2-amino-7-methyl-1,8-naphthyridine (AMND) in well-designed AP-containing DNA single/double strands. The primary mechanism is discovered, showing that AMND only targets cytosine to form a pseudo-base pair, and therefore, fluorescence quenching of AMND arises through the DNA-mediated electron transfer (ET) between excited state AMND* and flanking nucleobases, most favorably with flanking guanines. Subtle dynamic conformational variations induced by different flanking nucleobases are revealed and found to modulate efficiencies of electron transfer and fluorescence quenching. These findings provide critical mechanistic insights for guiding the design of photoinduced electron transfer (PET)-based fluorescent ligands as sensitive single-base recognition reporters.

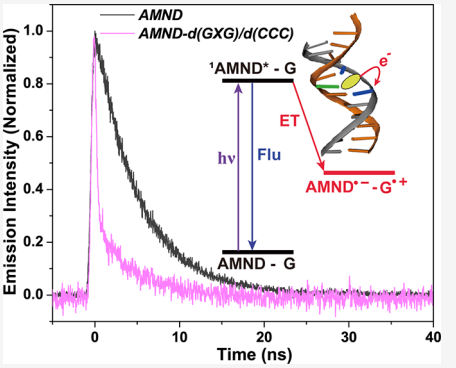

The abasic site (AP), as one of the most common forms of DNA damages while naturally occurring,[1] can provide the DNA duplex with a unique binding pocket, which allows for a direct contact of ligands with the target nucleobases.[2−5] By incorporation of a chemically stable AP site in a probe DNA to orient the AP site toward a target nucleobase, Teramae et al. implemented an unprecedented strategy of the ligand-based fluorescence assay for the single-nucleotide polymorphism (SNP) type for the first time.[2] Since then, studies on the nucleobase recognition based on interactions of the target nucleobases with the small fluorescent ligands trapped in the abasic site have attracted much attention.[4−11] The key idea of this method is that different fluorescence response signals will be generated after the pairing of the fluorescent ligand with different target nucleobases opposite the abasic site. For instance, 2-amino-7-methyl-1,8-naphthyridine (AMND, seen in Figure 1) shows significant fluorescence quenching when a cytosine base is placed opposite the abasic site, in comparison to the negligible fluorescence quenching when guanine is on the opposite.[2] The fluorescence emission behavior dependent upon the target nucleobase endows AMND with an ability to detect the cytosine/guanine mutation, which has been applicable to the sequence analysis of the cancer repression gene p53.[2,12] Until now, a set of heterocyclic compounds has been successfully developed to recognize target adenine,[6,7] thymine,[4,5,9] guanine,[13] and cytosine,[2,3,9] respectively.

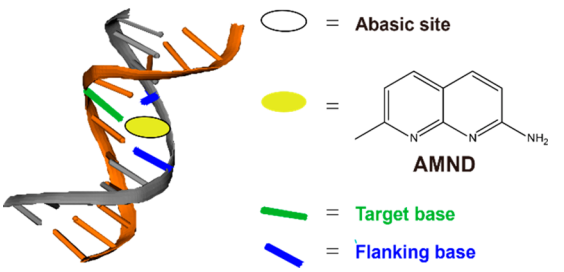

Figure 1. Schematic illustration of nucleobase recognition via interactions between AMND and the abasic-site-containing DNA duplexes.

The striking features of the fluorescent ligand in nucleobase recognition have posed particular interest in understanding the underlying molecular mechanisms. Structural characterization of nuclear magnetic resonance (NMR) experiments proved that the formation of hydrogen bonds between AMND and C is likely the reason for the highly selective binding.[14]

Received: August 3, 2023
Revised: October 21, 2023
Accepted: November 14, 2023
Published: November 17, 2023

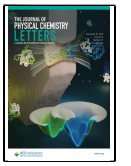

Meanwhile, the melting temperature experiments indicated that the stacking of AMND with the flanking G base at the AP site also plays an important role in the binding stability.[2] However, the key aspects governing the nucleobase recognition mechanism, i.e., why the fluorescence quenching depends upon the target nucleobase, is still unclear. Therefore, investigations of the fluoresence quenching dynamics through time-resolved spectroscopy measurements become indispensable for the establishment of target nucleobase recognition methods based on the AP-site-containing DNA/fluorescence ligand probe.

Here, we perform fluorescence dynamic studies for AMND trapped in abasic-site-containing DNA by means of the time-correlated single photon counting (TCSPC) method. A tetrahydrofuranyl residue (dSpacer) is used to incorporate the abasic site in the 11-mer oligodeoxynucleotides (ODNs, 5′-TCCA**NXN**CAAC-3′, where X = dSpacer and N = flanking bases).[2] The fluorescence quenching lifetimes of AMND in response to the altering of nucleobases opposite the abasic site and the flanking nucleobases at the abasic site have been thoroughly examined. A primary mechanism of DNA-mediated electron transfer between the excited state AMND (AMND*) and the flanking nucleobases, most favorably for AMND* with guanines, is established unambiguously. Moreover, the pseudo-base-pairing interaction of AMND with cytosine is shown to be the origin of target C base recognition, which accommodates AMND into the AP cavity to stack with flanking guanine bases and then facilitates the occurrence of electron transfer. Subtle dynamic conformational variations induced by the different flanking nucleobases are revealed and found to modulate the interactions between the electronic donor and the acceptor, thereby affecting efficiencies of electron transfer and fluorescence quenching. These investigations reveal not only the mechanism of nucleobase recognition through fluorescence quenching of small ligands, such as AMND, but also how conformational heterogeneity within such DNA/ligand complexes affects the key electron transfer dynamics, thus providing a core foundation for developing photoinduced electron transfer (PET)-based fluorescence ligands as dual reporters of the DNA base sequence and base dynamics.

First, the steady-state fluorescence quenching of AMND by four different nucleotides in bulk solution is examined, as shown in Figure 2. To avoid reabsorption and re-emission (inner filter effects),[15] the concentration of AMND is kept low at micromolar level. Free AMND in solution exhibits a strong fluorescence peak at 403 nm. There is no obvious change in the fluorescence intensity after adding dAMP, dTMP, and dCMP with the concentration in the range of 0.0−0.1 mM. However, the fluorescence intensity of AMND is obviously reduced upon the addition of dGMP, which strictly follows a linear concentration dependence in the Stern−Volmer plot (Figure 2). In general, excited state energy transfer or electron transfer is responsible for the fluorescence quenching.[15] Because the emission spectrum of AMND (λ_{max} = 403 nm) does not overlap with the absorption spectra of nucleobases (λ_{max} = 260 nm), in other words, the emission energy of AMND is below the absorption energy of nucleobases, energy transfer between excited state AMND* and nucleobases can be ruled out immediately.

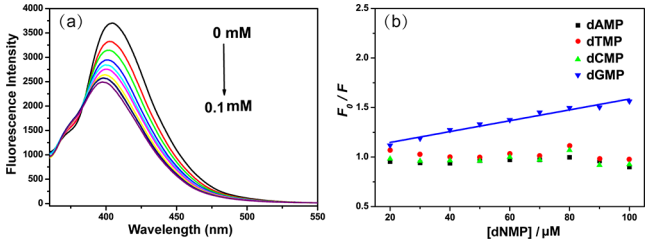

Figure 2. (a) Fluorescence spectra of AMND in the absence (black line) and presence (chromatic lines) of an increased concentration of dGMP. (b) Stern−Volmer plots of AMND quenched by dNMP in water (N = adenine, thymine, guanine, and cytosine). [AMND] = 1 μM, $[dNMP]_{max}$ = 0.1 mM, excitation wavelength λ_{ex} = 343 nm, and emission wavelength λ_{em} = 403 nm.

The possibility of electron transfer from the nucleobase to AMND* is further assessed by calculating the standard free energy change (ΔG^0) (Table S1 of the Supporting Information) using the Rehm−Weller equation (eq 1).[16] Cyclic voltammogram experiments were performed to obtain the redox potential of AMND (Figure S1 of the Supporting Information). The oxidation potentials of nucleobases guanine (G, +1.49 V), adenine (A, +1.96 V), thymine (T, +2.11 V), and cytosine (C, +2.14 V) are from ref 17. ΔE_{00} is the energy difference between the ground state and excited electronic state obtained from the intersection of the normalized absorption and fluorescence emission spectra. ΔH_{solv} is a coulombic term relating the energy of the separated ions (~0.06 eV in buffer solution).[16,18]

$$\Delta G^0 = E^0_{D^{\bullet+}/D} - E^0_{A/A^{\bullet-}} - \Delta E_{00}(A) - \Delta H_{solv} \quad (1)$$

Given that dGMP has the lowest redox potential and exhibits the most obvious quenching effect among the four nucleobases, the electron donor should be the nucleobase and the electron acceptor is the excited state AMND*. Obviously, ΔG^0 is negative (−0.17 eV) only for G but becomes positive for A (+0.30 eV), T (+0.45 eV), and C (+0.48 eV), which agrees with the fluorescence quenching experiments. Hence, electron transfer can be regarded as the key to the fluorescence quenching of AMND, and guanine bases are the only thermodynamically feasible electron donor.

Second, time-resolved fluorescence responses of AMND in AP-containing DNA duplexes hybridized by 5′-TCCA**NXN**-CAAC-3′ (X = dSpacer and N = flanking bases) with its counterpart oligomer sequences (detailed sequences shown in Table S2 of the Supporting Information) were further investigated by TCSPC. The AP-containing duplexes abbreviated as ds-(GXG)/d(C**C**C) and ds-(GXG)/d(C**G**C) are examined in comparison to the single strands of ss-(GXG), ss-(CCC), and ss-(CGC) and the fully paired duplex of ds-(GGG)/d(CCC). The fluorescence decay dynamics of free AMND in solution and AMND in various DNA was monitored at its peak wavelength of 403 nm upon 370 nm ps laser excitation (Figure 3). For free AMND alone, the fluorescence follows a single-exponential decay, with a lifetime of 5.45 ns.

For AMND in the presence of various DNAs, some pertinent observations and facts are obtained. (i) Upon the addition of the single-strand ss-(GXG), ss-(CCC), and ss-(CGC), the fluorescence decay curves remain essentially unchanged relative to that for AMND alone, indicating that AMND does not bind with the single strands, not even with the ss-(GXG) with an AP site. Therefore, the single strands alone have no interaction with AMND and have little effect on the fluorescence behavior. (ii) For the double strands, efficient fluorescence quenching of AMND as evidenced by the

https://doi.org/10.1021/acs.jpclett.3c02170
J. Phys. Chem. Lett. 2023, 14, 10585−10591

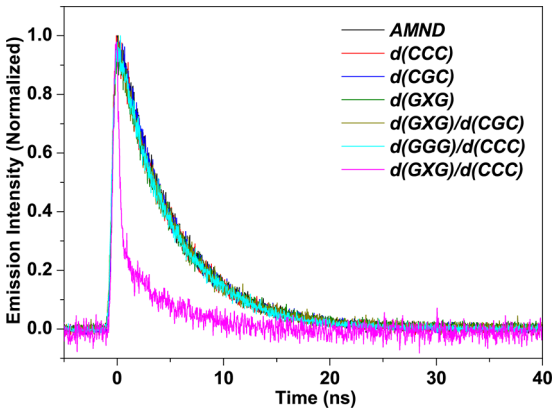

Figure 3. Normalized fluorescent decay curves of AMND in the absence (black lines) and presence (chromatic lines) of various DNA. [AMND] = 15 μM, [DNA] = 30 μM, λ_{ex} = 370 nm, λ_{em} = 403 nm, and 10 mM sodium cacodylate buffer containing 100 mM NaCl and 1 mM ethylenediaminetetraacetic acid (EDTA) at pH 7.0. Note that on the basis of the melting temperature analysis of abasic-site-containing DNA duplexes (Figure S2 of the Supporting Information), the experiments were performed at a low temperature (5 °C) to ensure the DNA stability.

dramatic decay acceleration is exclusively observed with d(GXG)/d(C**C**C), when cytosine is opposite the AP site (as the target base). In sharp contrast, the fluorescence decay remains unchanged when adding d(GXG)/d(C**G**C), with the target base being guanine. Obviously, there is a highly selective binding interaction of AMND with d(GXG)/d(C**C**C) as a result of the hydrogen bond formation of AMND solely with the target C base,[2,14] thus accommodating AMND into the AP cavity of d(GXG)/d(C**C**C). Then, AMND behaves like a paired base with C, overlapping with the two flanking guanine bases (Gs) of the AP-containing strand by the π-stacking interaction. Under such a binding configuration, the thermodynamically favorable electron transfer between excited state AMND* and flanking Gs thus occurs, leading to dramatic fluorescence quenching acceleration of AMND. As for d(GXG)/d(C**G**C), the target base guanine cannot pair with AMND through hydrogen bonds and, thus, cannot incorporate AMND into the AP cavity, causing no stacking with flanking Gs to allow for electron transfer and fluorescence quenching, although the heterocyclic guanine base is quite suitable for π stacking with the AMND molecule.[2] Therefore, the selective hydrogen-bonding interaction of the target C base with AMND is the prerequisite to promote the binding of AMND into the abasic cavity, which then facilitates the π stacking of AMND with flanking Gs in the AP-containing strand to cause their electronic coupling and ultimate fluorescence quenching by the electron transfer pathway. (iii) A further comparative experiment was performed, showing that the fluorescence decay kinetics of AMND is not affected at all when adding the fully paired double-strand ds-(GGG)/d(CCC). Although some planar π-conjugate fluorescent molecules can intercalate into base pairs of DNA duplexes by π-stacking interactions,[19,20] our results here reveal that the AMND molecule cannot intercalate into base pairs in common dsDNA without abasic sites. Thus, there is a lack of electron transfer and lack of fluorescence quenching when adding common ds-DNA. Altogether, these results indicate that AMND, as a probe for cytosine, can only function in ds-DNA with abasic sites and electron transfer from flanking guanine bases to excited state AMND* plays essential roles.

Upon complexation of AMND via hydrogen bonds with the target cytosine, fluorescence of AMND is quenched by electron transfer from flanking guanine bases. In comparison to guanine, which owns the lowest oxidation potential of 1.49 V,[17,21] other nucleobases, such as thymine, are not susceptible to offer electrons, as assessed by the ΔG^0 calculation above. The question arises concerning how the fluorescence of AMND would respond to the variation of nucleobases flanking the abasic site when the target base is C and AMND can be incorporated into the AP cavity. Figure 4a shows the

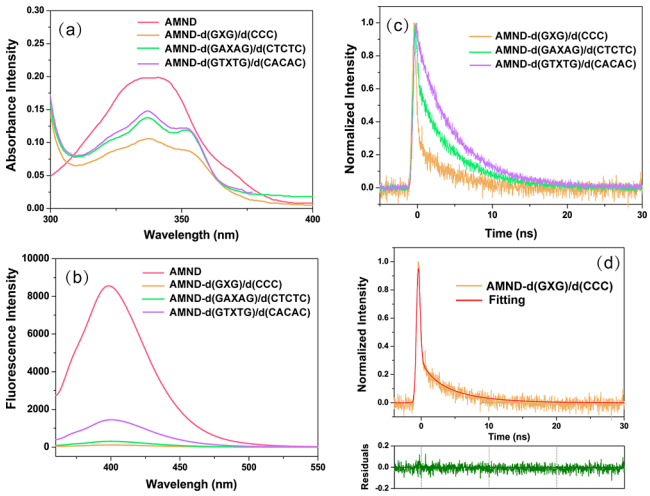

Figure 4. (a) Absorption spectra. (b) Fluorescence spectra of AMND in the absence and presence of abasic-site-containing DNA duplexes. (c) Normalized fluorescence decay profiles of the corresponding samples. [AMND] = 15 μM, [DNA] = 30 μM, λ_{ex} = 370 nm, λ_{em} = 403 nm, and 10 mM sodium cacodylate buffer containing 100 mM NaCl and 1 mM EDTA at pH 7.0 and 5 °C. (d) Fitting results for the fluorescence decay kinetics of AMND in d(**GXG**)/d(CCC).

absorption spectra of AMND upon the addition of the abasic-site-containing DNA duplexes with different flanking bases at 5 °C in pH 7.0 buffer solutions. The broad absorption band of AMND at 343 nm undergoes peak splitting, while the intensity decreases and the band becomes narrower, as a result of π-stacking interactions of AMND with flanking bases. The stacking geometry may result in a weaker oscillator strength responsible for the absorption reduction and formation of new absorption peaks that are related to a new electronic state transition.[20,22] Moreover, the decrease of absorption intensity of AMND follows the order d(**GXG**)/d(CCC) duplex > d(G**AXA**G)/d(CTCTC) duplex > d(G**TXT**G)/d(CACAC) duplex, implying that the degree of π-stacking interactions of AMND with flanking bases also follows the order guanine > adenine > thymine. Meanwhile, the steady-state fluorescence spectra were performed. As shown in Figure 4b, the fluorescence quenching of AMND upon the addition of abasic-site-containing DNA duplexes depends upon the flanking bases: the largest decrease is obtained for d(**GXG**)/d(CCC), and the quenching extent follows the order d(**GXG**)/d(CCC) > d(G**AXA**G)/d(CTCTC) > d-(G**TXT**G)/d(CACAC). The fluorescence decay dynamic measurements (Figure 4c) show the same quenching order. It is not surprising that d(**GXG**)/d(CCC) exhibits the strongest quenching effect, owing to the closest distance

https://doi.org/10.1021/acs.jpclett.3c02170
J. Phys. Chem. Lett. 2023, 14, 10585−10591

Table 1. Fluorescence Lifetimes of AMND in Three AP DNA Duplexes Obtained through Multi-exponential Fitting Analyzation[a]

	t_1 (ns)	percentage (%)	t_2 (ns)	percentage (%)	t_3 (ns)	percentage (%)
DNA1[b]		5	1.63 (±0.02)	3	0.12 (±0.01)	92
DNA2[c]	5.38 (±0.23)	18	3.20 (±0.15)	23	0.34 (±0.01)	59
DNA3[d]		49	4.96 (±0.18)	36	0.86 (±0.01)	15

[a]The fluorescence lifetimes of AMND in abasic-site-containing DNA duplexes are obtained from the fitting of convoluting the IRF with a triple-exponential decay function $[I(t) = A_1e^{-x/t_1} + A_2e^{-x/t_2} + A_3e^{-x/t_3}]$. Pre-exponential factors for the three lifetime components yield the respective percentages of three conformation states. The experimental condition is 10 mM sodium cacodylate buffer containing 100 mM NaCl and 1 mM EDTA at pH 7.0 and 5 °C. [b]DNA1 = d(**GXG**)/d(CCC), where flanking nucleobases are G. [c]DNA2 = d(G**AXA**G)/d(CTCTC), where flanking nucleobases are A. [d]DNA3 = d(G**TXT**G)/d(CACAC), where flanking nucleobases are T.

between electron donor guanine and acceptor AMND as well as the largest degree of π-stacking interactions of AMND with guanine.

For d(G**AXA**G)/d(CTCTC) and d(G**TXT**G)/d(CACAC), when the flanking base in the AP site is adenine or thymine, how does fluorescence quenching occur? Generally, it has been accepted that charges could migrate rapidly and over a significant distance through the DNA π stacking, and the extent of π stacking affects the electron transfer processes.[23−26] Inside DNA, nucleobases are regularly π-stacked with each other; therefore, the DNA-mediated electron transfer may exist. In the case of d(G**AXA**G)/d(CTCTC), although adenine cannot directly donate an electron to AMND* at the abasic site, the electrons could transfer from G to AMND* through the bridge base A. This also occurs in the case of d(G**TXT**G)/d(CACAC). Here, both the flanking adenine and thymine bases that have been exemplified as an excellent electron transfer channel[23−26] can bridge the guanine base (donor) and AMND* (acceptor), resulting in the fluorescence quenching of AMND* in d(G**AXA**G)/d(CTCTC) or d(G**TXT**G)/d(CACAC). Majima et al. reported that electron transfer along the DNA strand is strongly affected by the highest occupied molecular orbital (HOMO) energy gap between G and the bridging bases.[26] The lower the gap, the faster the electron transfer rate. Considering the much smaller HOMO energy gap between G and A (0.26 eV) than that for G and T (0.78 eV), adenine is more efficient than thymine for bridging the electron transfer for guanine and AMND*. Thus, the observed fluorescence quenching of AMND in d(G**TXT**G)/d(CACAC) is much weaker than that in d(G**AXA**G)/d(CTCTC), and this difference is also reflected in the electron transfer rates (Table 1) for these two sequences.

Furthermore, the electron transfer in the DNA duplexes can be modulated by not only the static base stacking but also the base conformation dynamics (dynamic base motions). It was reported that the fluorescence decay of 2-aminopurine had a clear response to the base flipping, which largely increased the amplitude of the long-lifetime component of 2-aminopurine complexed in the M.HhaI DNA.[27,28] Enlightened by this, we dissect the fluorescence decay dynamics of AMND in the abasic-site-containing DNA duplexes. As shown in panels c and d of Figure 4 and Figures S3 and S4 of the Supporting Information, the most satisfactory fitting results can be obtained by convoluting the instrument response function (IRF) with a three-exponential function $[I(t) = A_1e^{-x/t_1} + A_2e^{-x/t_2} + A_3e^{-x/t_3}]$. The fitting parameters are summarized in Table 1. Obviously, AMND showed three fluorescence lifetime components in the presence of a basic-site-containing DNA duplexes. The longest lifetime components for the three duplexes are all 5.38 ns, which is identical to the fluorescence lifetime for the free AMND (5.45 ns). The shortest lifetime component equals 0.12 ns with d(**GXG**)/d(CCC), 0.34 ns with d(G**AXA**G)/d(CTCTC), and 0.86 ns with d(G**TXT**G)/d(CACAC). The intermediate lifetime component is 1.63 ns with d(**GXG**)/d(CCC), 3.2 ns with d(G**AXA**G)/d(CTCTC), and 4.96 ns with d(G**TXT**G)/d(CACAC). The multiple fluorescence decay lifetimes are the sensitive reports of the heterogeneous DNA environment, showing the existence of at least three conformational states around the abasic site for emitting AMND. Moreover, from the fitted pre-exponential factors, the relative amplitude of each conformational state can be obtained.

In the case of d(**GXG**)/d(CCC), the shortest component presents an emission lifetime of 120 ps, of which the relative amplitude is 92%. This dominant component could be identified as the well-stacked conformation of AMND with flanking G bases, in which the fluorescence is efficiently quenched by electron transfer. The 120 ps lifetime corresponds to the electron transfer from the guanine base to AMND*. To support such assignment, we performed time-dependent density-functional theory [(TD)DFT] calculations and orbital analysis as adopted before for a similar DNA system.[10,29] As shown in Figure 5, we optimized the structure of AMND stacking with two adjacent G bases (G-AMND-G) in a planar

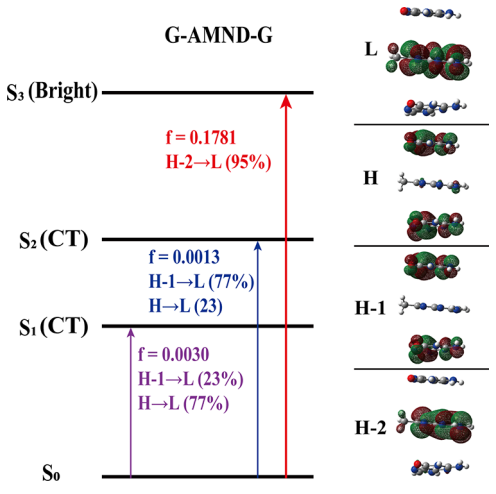

Figure 5. Jablonski diagram for singlet excited state transitions of G-AMND-G as determined by (TD)DFT calculations at the B3LYP/6-311+G* level with the solvent effect simulated by the polarizable continuum model (PCM). Carbon, oxygen, nitrogen, and hydrogen atoms are denoted with gray, red, blue, and white balls, respectively. Orbital amplitudes for HOMO-2 (H-2), HOMO-1 (H-1), HOMO (H), and LUMO (L) are also given.

https://doi.org/10.1021/acs.jpclett.3c02170
J. Phys. Chem. Lett. 2023, 14, 10585−10591

geometry, which could simplistically represent the well-stacked conformation of AMND in d(**GXG**)/d(CCC). For G-AMND-G, the ground state (S_0) to the third excited state (S_3) vertical transition [from HOMO-2 to lowest unoccupied molecular orbital (LUMO)] possesses a strong oscillator strength (f = 0.1781). This HOMO-2 to LUMO transition is similar to that of AMND alone (Figure S5 of the Supporting Information), and corresponds to the bright state emitting fluorescence. However, in G-AMND-G, strikingly, there are two lower lying states (S_2 and S_1), corresponding to the transitions of HOMO or HOMO-1 (with electron density mainly on flanking G) → LUMO (with electron density solely on AMND). These two transitions will result in electron transfer from G to AMND, which defines these (S_2 and S_1) as charge transfer (CT) states. Interestingly, our (TD)DFT calculations using the optimized geometry of AMND stacked between two adenines (A-AMND-A) or thymines (T-AMND-T) show that the HOMO and LUMO orbitals solely reside on the AMND moiety and there exists no CT state (Figure S5 of the Supporting Information). This corroborates our interpretation above that no direct electron transfer can occur for A with AMND or T with AMND upon excitation, and in −G**AXA**G− or −G**TXT**G− sequences, A or T serves as a bridging base for the electron transfer between G and AMND*.

For G-AMND-G, the two CT states are of a dark state character as a result of the small oscillator strength (f = 0.0030 for S_1 and 0.0013 for S_2). Besides, AMND is not a natural nucleobase, its insertion into the AP cavity may not enable the kind of weak intrinsic fluorescence of DNA duplexes as a result of collective nucleobase interaction.[30] The emission probability of the CT state for G-AMND-G must be extremely little. The observed fluorescence emission (λ_{max} = 403 nm) should stem from the bright state S_3 rather than the CT state. The relaxation of the S_3 state to the CT state, i.e., the electron transfer process, decreases the population in the S_3 state and results in the fluorescence decay with time. Thus, the accelerated fluorescence decay kinetics correspond to the electron transfer process.

Furthermore, using the orbital composition and energy, we calculated the electronic coupling (V = 0.0248 eV) between the electron acceptor (AMND) and donor (G) under well-stacked conformation on the basis of the fragment charge difference (FCD) method.[31] On the basis of the Marcus theory that has been extensively applied to understand inter- or intramolecular ET and ET in restricted hydrogen-bonded complexes,[32−37] using the obtained V (0.0248 eV), free energy change for electron transfer ΔG = −0.17 eV, and λ = 1 eV (a typical value of the reorganization energy in a polar solvent),[34,38] we estimated the electron transfer rate to be 93 ps for AMND with G in the well-stacked conformation of G-AMND-G. This predicted value is qualitatively consistent with the measured rate (120 ps) in d(**GXG**)/d(CCC), supporting the assignment of electron transfer from the guanine base to AMND*. It is worthwhile to mention that in d(**GXG**)/d(CCC), although AMND can form a pseudo-base pair with cytosine and insert into the AP cavity to stack with adjacent flanking G bases, AMND is not linked with other nucleobases by the sugar−phosphate backbone. Without the backbone alignment, the electronic interaction of AMND with G could be small. Thus, the electron transfer for ^{1}AMND* with G in AP-containing DNA can proceed much slower than the highly π-stacked collective behavior of the nucleobase−multimer system of a natural DNA duplex.[39,40] With the visualization of G-AMND-G as a chromophore fragment associated with the CT behavior, the energy of CT states could be stabilized further by solvation within the duplex structure, where the sequence and order of nucleobases along a given strand can determine the stability of this CT state in the whole duplex.[41] This leaves an open question for a professional theoretician to address.

Meanwhile, in d(**GXG**)/d(CCC), the longest component with a fluorescence lifetime of 5.38 ns similar to that of free AMND occupies only 5%, which should be assigned to AMND in an extra-helical environment: flipped-out AMND has a negligible stacking interaction with adjacent guanine bases and, thus, behaves as free AMND. Considering the high affinity of AMND pairing with target cytosines in abasic-site-containing DNA duplexes, the flipped-out AMND conformation hence makes a negligible contribution. Moreover, the third conformational state with an intermediate lifetime (around 1.63 ns) may belong to AMND imperfectly stacked with flanking bases, with also a negligible contribution to the fluorescence decay dynamics (less than 5%).

Similarly, the shortest lifetime component of 0.86 ns in d(G**TXT**G)/d(CACAC) should also be attributed to the well-stacked conformation of AMND with adjacent thymine bases. As a result of the longer electron transfer distance through the thymine bridge and the reductions of the stacking extent between AMND and thymine, this fluorescence lifetime is much longer than that in d(**GXG**)/d(CCC). Meanwhile, the relative amplitude of such a well-stacked conformation is reduced to 15%, while the longest lifetime component as a result of the flipped-out conformation turns out to be dominant (49%). These results indicate that AMND molecules are inclined to flip out of the abasic site pocket in d(G**TXT**G)/d(CACAC), preventing the efficient fluorescence quenching of AMND by electron transfer. Obviously, the less favorable π-stacking effects between AMND and thymine cannot render a rigid helix for AMND with thymine in the abasic site compared to that with guanine. Instead, flexible base motions are expected to be more favorable, and thus, the flipped-out conformation of AMND becomes dominant in d(G**TXT**G)/d(CACAC).

For AMND with d(G**AXA**G)/d(CTCTC), three components are also assigned to ET processes of the well-stacked, intermediate, and poorly stacked (flipped-out) conformations, respectively. Moreover, the double aromatic rings of flanking adenine are similar to guanine, which can enable the propensity of the well-stacked conformation with AMND for electron transfer to be dominant (59%), despite the substantial percentages of the intermediate (23%) and poorly stacked conformations (18%). Altogether, our time-resolved measurements reflect changes in not only electron transfer rates of AMND in different abasic-site-containing DNA duplexes but also dynamic conformational heterogeneity induced by the different flanking nucleobases, both of which are key aspects affecting efficiencies of fluorescence quenching behavior of AMND in recognizing target bases and should be considered when designing such nucleobase probe methodology.

In conclusion, we have systematically studied the fluorescence quenching dynamics of AMND in the abasic-site-containing DNA duplexes and ascertained the nucleobase recognition mechanism of the AP-site-containing DNA/fluorescence ligand probe. The experiments show that AMND selectively targets the cytosine base through pseudo-base pairing in the abasic site, and it cannot intercalate into

https://doi.org/10.1021/acs.jpclett.3c02170
J. Phys. Chem. Lett. 2023, 14, 10585−10591

common fully matched GC base pairs without abasic sites. Therefore, the fluorescence quenching of AMND can be successfully utilized for the detection of a single-base alternation related to cytosine, functioning as a DNA sequence probe. Meanwhile, we find that it is the electron transfer from flanking guanine bases to excited state AMND* that plays essential roles leading to such fluorescence quenching of AMND and the flanking bases have a great influence on electron transfer efficiencies. The flanking guanine base can undergo direct electron transfer to AMND*, with the largest propensity to form the π-stacking conformation with AMND, thus leading to the most efficient electron transfer (120 ps) and fluorescence quenching, whereas the flanking adenine and thymine bases can act as an electron transfer channel for bridging the guanine base (donor) and AMND* (acceptor) and have poorer π-stacking interaction with AMND, thus causing less efficient electron transfer pathways. Our time-resolved measurements reveal that, in abasic-site-containing DNA duplexes, the fluorescence response of excited AMND depends upon both the static π-stacking effects and dynamic conformation states related to the interactions between AMND and the flanking bases. To our knowledge, it is the first time that dynamics studies of fluorescence ligands have been reported in abasic-site-containing DNA duplexes. Moreover, our experimental results demonstrate that conformational diversities caused by base motions play an important role in fluorescence quenching of the AMND moiety. At any rate, our results clearly emphasize the importance of carefully considering the redox property and π-stacking conformation of flanking nucleobases in addition to their pseudo-base-pairing capability when rationally designing the PET-based fluorescent ligands as single-base recognition reporters.

■ ASSOCIATED CONTENT

Supporting Information

The Supporting Information is available free of charge at https://pubs.acs.org/doi/10.1021/acs.jpclett.3c02170.

Materials and methods, supporting figures and tables, and additional references (PDF)

■ AUTHOR INFORMATION

Corresponding Authors

Jialong Jie − *College of Chemistry, Beijing Normal University, Beijing 100875, People's Republic of China*; Email: jialong@bnu.edu.cn

Hongmei Su − *College of Chemistry, Beijing Normal University, Beijing 100875, People's Republic of China*; orcid.org/0000-0001-7384-6523; Email: hongmei@bnu.edu.cn

Authors

Chunfan Yang − *College of Chemistry, Beijing Normal University, Beijing 100875, People's Republic of China*

Fang Wang − *College of Chemistry, Beijing Normal University, Beijing 100875, People's Republic of China*

Qian Zhou − *College of Chemistry, Beijing Normal University, Beijing 100875, People's Republic of China*

Complete contact information is available at: https://pubs.acs.org/10.1021/acs.jpclett.3c02170

Notes

The authors declare no competing financial interest.

■ ACKNOWLEDGMENTS

The authors acknowledge the financial support provided by the National Natural Science Foundation of China (Grants 21933005, 21727803, 22003005, and 21425313).

■ REFERENCES

(1) Demple, B.; Harrison, L. Repair of Oxidative Damage to DNA: Enzymology and Biology. *Annu. Rev. Biochem.* **1994**, *63*, 915−948.

(2) Yoshimoto, K.; Nishizawa, S.; Minagawa, M.; Teramae, N. Use of Abasic Site-Containing DNA Strands for Nucleobase Recognition in Water. *J. Am. Chem. Soc.* **2003**, *125*, 8982−8983.

(3) Nishizawa, S.; Yoshimoto, K.; Seino, T.; Xu, C.-Y.; Minagawa, M.; Satake, H.; Tong, A.; Teramae, N. Fluorescence detection of cytosine/guanine transversion based on a hydrogen bond forming ligand. *Talanta* **2004**, *63*, 175−179.

(4) Nishizawa, S.; Sankaran, N. B.; Seino, T.; Cui, Y.-Y.; Dai, Q.; Xu, C.-Y.; Yoshimoto, K.; Teramae, N. Use of vitamin B2 for fluorescence detection of thymidine-related single-nucleotide polymorphisms. *Anal. Chim. Acta* **2006**, *556*, 133−139.

(5) Zhao, C.; Dai, Q.; Seino, T.; Cui, Y.-Y.; Nishizawa, S.; Teramae, N. Strong and selective binding of amiloride to thymine base opposite AP sites in DNA duplexes: Simultaneous binding to DNA phosphate backbone. *Chem. Commun.* **2006**, 1185−1187.

(6) Rajendar, B.; Nishizawa, S.; Teramae, N. Alloxazine as a ligand for selective binding to adenine opposite AP sites in DNA duplexes and analysis of single-nucleotide polymorphisms. *Org. Biomol. Chem.* **2008**, *6*, 670−673.

(7) Ye, Z.; Rajendar, B.; Qing, D.; Nishizawa, S.; Teramae, N. 6,7-Dimethyllumazine as a potential ligand for selective recognition of adenine opposite an abasic site in DNA duplexes. *Chem. Commun.* **2008**, 6588−6590.

(8) Sankaran, N. B.; Sato, Y.; Sato, F.; Rajendar, B.; Morita, K.; Seino, T.; Nishizawa, S.; Teramae, N. Small-Molecule Binding at an Abasic Site of DNA: Strong Binding of Lumiflavin for Improved Recognition of Thymine-Related Single Nucleotide Polymorphisms. *J. Phys. Chem. B* **2009**, *113*, 1522−1529.

(9) Sato, Y.; Nishizawa, S.; Yoshimoto, K.; Seino, T.; Ichihashi, T.; Morita, K.; Teramae, N. Influence of substituent modifications on the binding of 2-amino-1,8-naphthyridines to cytosine opposite an AP site in DNA duplexes: Thermodynamic characterization. *Nucleic Acids Res.* **2009**, *37*, 1411−1422.

(10) Rajendran, A.; Zhao, C.; Rajendar, B.; Thiagarajan, V.; Sato, Y.; Nishizawa, S.; Teramae, N. Effect of the bases flanking an abasic site on the recognition of nucleobase by amiloride. *Biochim. Biophys. Acta, Gen. Subj.* **2010**, *1800*, 599−610.

(11) Nishizawa, S.; Sato, Y.; Teramae, N. Recent Progress in Abasic Site-binding Small Molecules for Detecting Single-base Mutations in DNA. *Anal. Sci.* **2014**, *30*, 137−142.

(12) Matozaki, T.; Sakamoto, C.; Matsuda, K.; Suzuki, T.; Konda, Y.; Nakano, O.; Wada, K.; Uchida, T.; Nishisaki, H.; Nagao, M.; Kasuga, M. Missense mutations and a deletion of the p53 gene in human gastric cancer. *Biochem. Biophys. Res. Commun.* **1992**, *182*, 215−223.

(13) Dai, Q.; Xu, C.-Y.; Sato, Y.; Yoshimoto, K.; Nishizawa, S.; Teramae, N. Enhancement of the Binding Ability of a Ligand for Nucleobase Recognition by Introducing a Methyl Group. *Anal. Sci.* **2006**, *22*, 201−203.

(14) Yoshimoto, K.; Nishizawa, S.; Koshino, H.; Sato, Y.; Teramae, N.; Maeda, M. Assignment of hydrogen-bond structure in a ligand-nucleobase complex inside duplex DNA: Combined use of quantum chemical calculations and ^{15}N NMR experiments. *Nucleic Acids Symp. Ser.* **2005**, *49*, 255−256.

(15) Lakowicz, J. R. *Principles of Fluorescence Spectroscopy*; Springer: Boston, MA, 2006; DOI: 10.1007/978-1-4757-3061-6.

(16) Rehm, D.; Weller, A. Kinetics of fluorescence quenching by electron and H-atom transfer. *Isr. J. Chem.* **1970**, *8*, 259−271.

(17) Seidel, C. A. M.; Schulz, A.; Sauer, M. H. M. Nucleobase-Specific Quenching of Fluorescent Dyes. 1. Nucleobase One-Electron

Redox Potentials and Their Correlation with Static and Dynamic Quenching Efficiencies. *J. Phys. Chem.* **1996**, *100*, 5541−5553.
(18) Rehm, D.; Weller, A. Kinetik und Mechanismus der Elektronübertragung bei der Fluoreszenzlöschung in Acetonitril. *Ber. Bunsen-Ges. Phys. Chem.* **1969**, *73*, 834−839.
(19) Fröbel, S.; Reiffers, A.; Torres Ziegenbein, C.; Gilch, P. DNA Intercalated Psoralen Undergoes Efficient Photoinduced Electron Transfer. *J. Phys. Chem. Lett.* **2015**, *6*, 1260−1264.
(20) Jiao, Z.; Yang, C.; Zhou, Q.; Hu, Z.; Jie, J.; Zhang, X.; Su, H. Sequence-specific binding behavior of coralyne toward triplex DNA: An ultrafast time-resolved fluorescence spectroscopy study. *J. Chem. Phys.* **2023**, *158*, 045101.
(21) Steenken, S.; Jovanovic, S. V. How Easily Oxidizable Is DNA? One-Electron Reduction Potentials of Adenosine and Guanosine Radicals in Aqueous Solution. *J. Am. Chem. Soc.* **1997**, *119*, 617−618.
(22) Song, D.; Yang, W.; Qin, T.; Wu, L.; Liu, K.; Su, H. Explicit Differentiation of G-Quadruplex/Ligand Interactions: Triplet Excited States as Sensitive Reporters. *J. Phys. Chem. Lett.* **2014**, *5*, 2259−2266.
(23) Giese, B.; Amaudrut, J.; Köhler, A.-K.; Spormann, M.; Wessely, S. Direct observation of hole transfer through DNA by hopping between adenine bases and by tunnelling. *Nature* **2001**, *412*, 318−320.
(24) Pascaly, M.; Yoo, J.; Barton, J. K. DNA Mediated Charge Transport: Characterization of a DNA Radical Localized at an Artificial Nucleic Acid Base. *J. Am. Chem. Soc.* **2002**, *124*, 9083−9092.
(25) Fujitsuka, M.; Majima, T. Hole and excess electron transfer dynamics in DNA. *Phys. Chem. Chem. Phys.* **2012**, *14*, 11234−11244.
(26) Kawai, K.; Hayashi, M.; Majima, T. HOMO energy gap dependence of hole-transfer kinetics in DNA. *J. Am. Chem. Soc.* **2012**, *134*, 4806−4811.
(27) Jean, J. M.; Hall, K. B. 2-Aminopurine fluorescence quenching and lifetimes: Role of base stacking. *Proc. Natl. Acad. Sci. U. S. A.* **2001**, *98*, 37−41.
(28) Neely, R. K.; Daujotyte, D.; Grazulis, S.; Magennis, S. W.; Dryden, D. T. F.; Klimašauskas, S.; Jones, A. C. Time-resolved fluorescence of 2-aminopurine as a probe of base flipping in M.HhaI−DNA complexes. *Nucleic Acids Res.* **2005**, *33*, 6953−6960.
(29) Hardman, S. J. O.; Thompson, K. C. Influence of Base Stacking and Hydrogen Bonding on the Fluorescence of 2-Aminopurine and Pyrrolocytosine in Nucleic Acids. *Biochemistry* **2006**, *45*, 9145−9155.
(30) Gustavsson, T.; Markovitsi, D. Fundamentals of the Intrinsic DNA Fluorescence. *Acc. Chem. Res.* **2021**, *54*, 1226−1235.
(31) Voityuk, A. A.; Rösch, N. Fragment charge difference method for estimating donor−acceptor electronic coupling: Application to DNA π-stacks. *J. Chem. Phys.* **2002**, *117*, 5607−5616.
(32) Lewis, F. D.; Kalgutkar, R. S.; Wu, Y.; Liu, X.; Liu, J.; Hayes, R. T.; Miller, S. E.; Wasielewski, M. R. Driving Force Dependence of Electron Transfer Dynamics in Synthetic DNA Hairpins. *J. Am. Chem. Soc.* **2000**, *122*, 12346−12351.
(33) Fukuzumi, S.; Nishimine, M.; Ohkubo, K.; Tkachenko, N. V.; Lemmetyinen, H. Driving Force Dependence of Photoinduced Electron Transfer Dynamics of Intercalated Molecules in DNA. *J. Phys. Chem. B* **2003**, *107*, 12511−12518.
(34) Reid, G. D.; Whittaker, D. J.; Day, M. A.; Turton, D. A.; Kayser, V.; Kelly, J. M.; Beddard, G. S. Femtosecond Electron-Transfer Reactions in Mono- and Polynucleotides and in DNA. *J. Am. Chem. Soc.* **2002**, *124*, 5518−5527.
(35) Lewis, F. D.; Liu, X.; Miller, S. E.; Hayes, R. T.; Wasielewski, M. R. Dynamics of Electron Injection in DNA Hairpins. *J. Am. Chem. Soc.* **2002**, *124*, 11280−11281.
(36) Rosspeintner, A.; Angulo, G.; Vauthey, E. Bimolecular Photoinduced Electron Transfer Beyond the Diffusion Limit: The Rehm−Weller Experiment Revisited with Femtosecond Time Resolution. *J. Am. Chem. Soc.* **2014**, *136*, 2026−2032.
(37) Miller, J. R.; Calcaterra, L. T.; Closs, G. L. Intramolecular long-distance electron transfer in radical anions. The effects of free energy and solvent on the reaction rates. *J. Am. Chem. Soc.* **1984**, *106*, 3047−3049.
(38) Steenkeste, K.; Enescu, M.; Tfibel, F.; Perrée-Fauvet, M.; Fontaine-Aupart, M.-P. Ultrafast Guanine Oxidation by Photoexcited Cationic Porphyrins Intercalated into DNA. *J. Phys. Chem. B* **2004**, *108*, 12215−12221.
(39) Kwok, W.-M.; Ma, C.; Phillips, D. L. Bright" and "Dark" Excited States of an Alternating AT Oligomer Characterized by Femtosecond Broadband Spectroscopy. *J. Phys. Chem. B* **2009**, *113*, 11527−11534.
(40) Borrego-Varillas, R.; Cerullo, G.; Markovitsi, D. Exciton Trapping Dynamics in DNA Multimers. *J. Phys. Chem. Lett.* **2019**, *10*, 1639−1643.
(41) Martínez Fernández, L.; Santoro, F.; Improta, R. Nucleic Acids as a Playground for the Computational Study of the Photophysics and Photochemistry of Multichromophore Assemblies. *Acc. Chem. Res.* **2022**, *55*, 2077−2087.

https://doi.org/10.1021/acs.jpclett.3c02170
J. Phys. Chem. Lett. 2023, 14, 10585−10591